Environ. Sci. Technol. **1998**, *32,* 1588−1595

Mechanism of the Degradation of 1,4-Dioxane in Dilute Aqueous Solution Using the UV/Hydrogen Peroxide Process

MIHAELA I. STEFAN AND
JAMES R. BOLTON*
Photochemistry Unit, Department of Chemistry,
The University of Western Ontario, London,
Ontario, Canada N6A 5B7

1,4-Dioxane is an EPA priority pollutant often found in contaminated groundwaters and industrial effluents. The common techniques used for water purification are not applicable to 1,4-dioxane, and the currently used method (distillation) is laborious and expensive. This study aims to understand the degradation mechanism of 1,4-dioxane and its byproducts in dilute aqueous solution toward complete mineralization, by using the UV/H_2O_2 process in a UV semibatch reactor. The decay of 1,4-dioxane generated several intermediates identified and quantified as aldehydes (formaldehyde, acetaldehyde, and glyoxal), organic acids (formic, methoxyacetic, acetic, glycolic, glyoxylic, and oxalic) and the mono- and diformate esters of 1,2-ethanediol. Measurement of the total organic carbon (TOC) during the treatment indicated a good agreement between the experimentally determined TOC values and those calculated from the quantified reaction intermediates, ending in complete mineralization. A reaction mechanism, which accounts for the observed intermediate products and their time profiles during the treatment, is proposed. Considering the efficacy of the 1,4-dioxane removal from dilute aqueous solutions, as shown in this work, the present study can be regarded as a model for industrially affordable Advanced Oxidation Technologies.

Introduction

1,4-Dioxane or diethylene dioxide is a frequently used solvent for organic compounds (*1*) and, thus, is widely used in industry. 1,4-Dioxane causes liver damage and kidney failure, has been shown to be carcinogenic to animals, and is a potential carcinogen for humans (*2*) and, hence, is classified as a hazardous waste and a priority pollutant. 1,4-Dioxane falls under the regulations of the Environmental Protection Agency (EPA), which has set a discharge limit of 30 μg L^{-1}.

1,4-Dioxane is a recalcitrant molecule to biodegradation under conventional biotreatment technologies (*3*, *4*), but relatively recent studies have revealed enhanced biodegradation rates under certain aerobic conditions when combined with an advanced oxidation process pretreatment (*5*, *6*). Adsorption on activated carbon and air-stripping techniques cannot remove 1,4-dioxane from water because of its high solubility and low vapor pressure.

Despite so many concerns regarding the removal of 1,4-dioxane from contaminated waters and the laborious and expensive conventional distillation method currently used, only a few treatment studies in aqueous solution have been reported in the literature.

Klecka and Gonsoir (*7*) studied the incomplete chemical oxidation of 1,4-dioxane by chlorine (as NaClO) and by Fenton's reagent. Adams et al. (*6*) used the O_3/H_2O_2 process to remove 1,4-dioxane and enhance its biodegradability. Recently, two papers have been published on the degradation of 1,4-dioxane by TiO_2 photocatalysis (*8*, *9*). In each case, the principal intermediate found was 1,2-ethanediol diformate ester. All of the above processes involve generation of $^{\bullet}OH$ radicals with low efficiency compared to the UV/H_2O_2 process (quantum yield of 1.0).

Photoinduced oxidation methods using UV light and added H_2O_2, a branch of Advanced Oxidation Technologies, have proven to be very efficient for the removal of toxic organic pollutants found in the aquatic environment. Since the 1960s, a few reports have mentioned the oxidizing ability of the UV/H_2O_2 system (*10*−*12*), but during the past decade this process has attracted extensive attention as a modern technology for ground or wastewater purification (*13*) and has been studied for a wide range of hazardous organic compounds (*14*−*29*).

Several studies have examined the photochemistry of 1,4-dioxane either in neat liquid (*30*−*34*) or in aqueous solution (*35*, *36*), but only a patent publication reports the degradation of 1,4-dioxane sensitized by the UV photolysis of H_2O_2 (*37*). The authors reported 88−94% removal of the initial concentration of 1,4-dioxane after 60 min of irradiation, but no systematic study of intermediates or reaction pathways was explored.

The present work was undertaken with the aim of understanding of the mechanism of 1,4-dioxane degradation in dilute aqueous solution induced by the photolysis of hydrogen peroxide. The decay of 1,4-dioxane and the time profiles of the intermediates generated during the treatment have been followed until complete mineralization has been achieved. A reaction mechanism has been proposed that accounts for the observed experimental data.

Experimental Section

Reagents and Materials. 1,4-Dioxane (Fisher certified ACS grade) and hydrogen peroxide (30%, Caledon, analytical reagent grade) were used as received. The organic acids and aldehydes (analytical reagent grade) were used without any further purification. Catalase from bovine liver was obtained from Sigma.

The mono- and diformate esters of 1,2-ethanediol are not commercially available and were synthesized from 5.2 mL of ethylene bromide (Fisher, certified), 3.3 mL of formic acid (99%, Sigma, analytical reagent grade) and 4.8 g of sodium formate (Fisher, certified) refluxed for 30 h. After salt filtration, the residual formic acid and ethylene bromide were removed by vacuum distillation. The ester mixture was extracted into dried ethyl ether, which was then removed by vacuum distillation. All operations were carried out carefully avoiding any contact with water. The final reaction mixture contained 72% 1,2-ethanediol diformate and 27% 1,2-ethanediol monoformate, as determined by both GC/MS and NMR.

Deionized water was used in all experiments and analytical determinations.

Apparatus. The Rayox reactor (provided by Calgon Carbon Oxidation Technologies of Markham, Ontario, Canada) has been described elsewhere (*24*). The photon flux entering the 6 L reactor from the UV−vis lamp was (5.59

---

* Corresponding author e-mail: jbolton@julian.uwo.ca; telephone: (519)661-2170; fax: (519)661 3022.

S0013-936X(97)00633-0 CCC: $15.00

© 1998 American Chemical Society
Published on Web 04/17/1998

± 0.14) × 10^{-4} einstein s^{-1} in the wavelength range 200−400 nm, as estimated from potassium ferrioxalate actinometry (*38*) and the spectral emission profile of the 1 kW Hg lamp provided by Calgon Carbon Oxidation Technologies. The fraction of UV light absorbed within 200−400 nm range by hydrogen peroxide and by 1,4-dioxane, individually, was calculated by using a previously developed computer model (*24*).

In all experiments, the reaction volume was 28 L, recirculated at 110 L min^{-1} from the reservoir to the UV reactor. Samples were taken downstream from the UV reactor after various exposure times.

The pH (Cole-Palmer model 5938-10 pH meter with a 5938-60 probe) and dissolved oxygen (ATI Orion model 840 DO meter) were measured with probes in the reservoir.

Analytical Determinations. Analytical measurements were performed on samples taken before irradiation and after certain exposure times.

1,4-Dioxane and the formate esters of 1,2-ethanediol were determined by using a Perkin-Elmer (Sigma 2B) Gas Chromatograph equipped with a FID and a high-performance DB 624 glass capillary column (30 m × 0.53 mm, 3.0 μm film thickness, J&W Scientific) and the following experimental conditions: injector temperature 250 °C, column temperature isocratic at 90 °C, detector temperature 300 °C, and carrier gas (helium) pressure at the column 90 kPa. With these settings, the following retention times were obtained: 1.48 min (1,4-dioxane), 3.55 min (1,2-ethanediol monoformate), and 3.78 min (1,2-ethanediol diformate). A Hewlett-Packard HP 3396 Series II integrator was employed to record the retention times and peak area data from the GC detector.

The 1,2-ethanediol formate esters were identified in the irradiated samples by using solid-phase microextraction (SPME) coupled with GC/MS. The method involved exposing the SPME 85 μm polyacrylate coating fiber (Supelco) to a salted solution vigorously stirred for 30 min. The desorption temperature in the GC injector was 250 °C. A GC temperature program was developed in connection with an ion trap MS detector.

Hydrogen peroxide was analyzed by the triiodide method (*39*). The spectrophotometric measurements were performed by using a Hewlett-Packard 8450A Diode Array Spectrophotometer and a 1 cm path quartz cell.

Organic acids were identified and quantified by ion-exchange separation combined with conductivity detection performed with a Dionex DX-100 Ion Chromatograph equipped with an anion self-regenerating suppressor ASRS-I and the AI-450 software program. Two different sets of IC conditions were developed depending on the nature of acids analyzed. Methoxyacetic, glyoxylic, malonic, and oxalic acids were analyzed using an IonPac AS 10 (4 × 250 mm) ion-exchange column (Dionex) coupled with an AG 10 guard column and a 80 mM NaOH eluent solution in deionized water, at an isocratic flow rate of 1 mL min^{-1}. Under these conditions, the acids mentioned above eluted at 3.0, 5.75, 15.05, and 18.4 min, respectively. In such a strong basic eluent, the 1,2-ethanediol formate esters hydrolyze to formic acid and 1,2-ethanediol during the elution contact times providing misleading determinations of the free formic acid. Moreover, glyoxal is converted to glycolic acid on the column interfering with the determination of free glycolic acid. Acetic acid and glycolic acid coelute under the above conditions.

Glycolic, acetic, and formic acids were analyzed on an IonPac AS 14 (4 × 250 mm) ion-exchange column preceded by an AG 14 guard column and using a 3 mM sodium tetraborate solution as an eluent at an isocratic flow of 1.45 mL min^{-1}. The retention times were 3.65, 3.85, and 4.15 min, respectively.

H_2O_2 was destroyed in the samples before analysis by the addition of 5 μL of 0.5% catalase aqueous solution into a 10 mL sample.

Aldehydes were identified by thin-layer chromatography and quantitatively determined as hydrazones by an HPLC method (*40*). The following retention times were observed for the quantified hydrazones: 2.35 min (formaldehyde), 3.5 min (acetaldehyde), and 12 min (glyoxal). A few minor peaks corresponding to some unidentified hydrazones have been also integrated at 4.7, 5.3, and 6.3 min. Formaldehyde was also estimated by the Nash method (*41*), and the results agreed very well with the HPLC measurements.

Total organic carbon (TOC) was determined using a Shimadzu TOC-5050 analyzer provided with an integrated ASI-5000-S autosampler.

Results and Discussion

Hydrogen peroxide and 1,4-dioxane are very weak absorbers of UV light. Under the conditions of the experiment (1 mM 1,4-dioxane and 15 mM H_2O_2), 50.8% of the UV light entering the reactor is absorbed by hydrogen peroxide, whereas only 0.15% is absorbed by 1,4-dioxane. Therefore, no direct photolysis of 1,4-dioxane should be expected.

1,4-Dioxane Degradation and Reaction Intermediates. Figure 1 shows the results of the UV/H_2O_2 treatment in aqueous solution.

Sensitized by direct photolysis of hydrogen peroxide, 1,4-dioxane decays rapidly following pseudo-first-order kinetics with an observed rate constant of $k = (8.7 \pm 0.4) \times 10^{-3}\ s^{-1}$, much higher than that determined for its direct photolysis [$k = (6.4 \pm 0.3) \times 10^{-5}\ s^{-1}$] under the same conditions. Within the first 5 min of irradiation, almost 90% of the initial concentration of 1,4-dioxane was depleted, while four major primary reaction intermediates, namely 1,2-ethanediol mono- and diformate esters, formic acid, and methoxyacetic acid were generated. According to the dynamics of the irradiated system depicted in Figure 1, panels a and b, these byproducts undergo further oxidative degradation initiated by $^{\bullet}OH$ radicals, leading to glycolic and acetic acids, and finally to oxalic acid as the last intermediate. A small amount of glyoxylic acid, reaching a maximum steady-state concentration of ~0.075 mM by 12 min exposure time and traces of malonic acid at maximum levels as high as ~0.015 mM by 15 min irradiation, was measured as well. The time profiles of some aldehydes identified and quantified in the studied system are presented in Figure 1c. They are the precursors of the corresponding acids mentioned above. Due to their high oxidation rates and high rate constants with hydroxyl radicals, the aldehydes reach only low concentrations in such a strongly oxidizing medium.

During the experiment, the pH dropped rapidly from 5.0 ($t = 0$ min) to 3.25 ($t = 12$ min), then slowly to a minimum of 3.12 ($t = 23$ min), and then increased gradually up to 4.2 by the end of the irradiation period ($t = 60$ min). This variation is consistent with the formation of the organic acids and their subsequent total removal through oxidation reactions. The lower pH at the end of experiment, compared to its initial value, is explained by dissolved CO_2 generated during the mineralization processes.

The level of O_2 decreased sharply from 0.24 mM ($t = 0$ min) to ~0.020 mM ($t = 3$ min) reaching a steady-state concentration at this level until $t = 12$ min, and then increased and reached a plateau value of ~0.70 mM by 35 min of irradiation (see also Figures 1 and 3). The first stage corresponds to the rapid oxidation of the parent molecule and the formation and then the decay of highly oxygenated intermediates, whereas the later oxygen increase is associated with a lower consumption of O_2 and the generation of oxygen from the photodecomposition of H_2O_2.

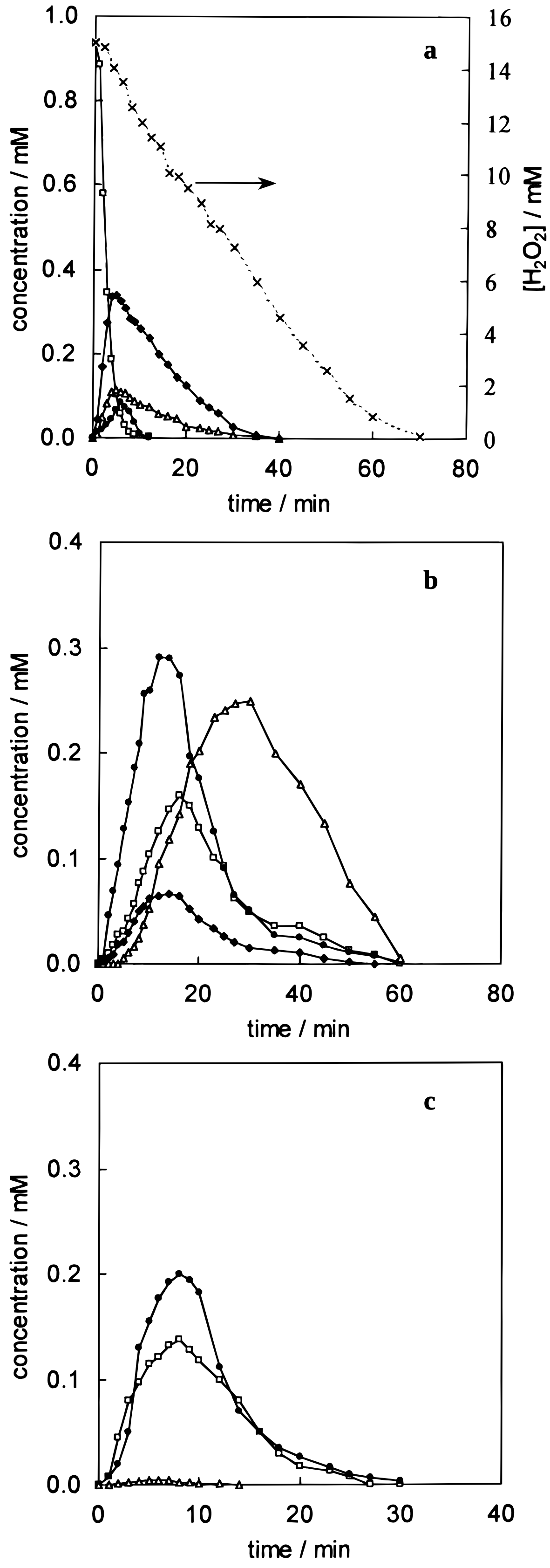

FIGURE 1. Time profiles during the UV/H_2O_2 treatment of 1,4-dioxane and its reaction intermediates: (a) 1,4-dioxane (□); H_2O_2 (×); 1,2-ethanediol diformate (◆); 1,2-ethanediol monoformate (△); methoxyacetic acid (●); (b) acetic acid (□); glycolic acid (◆); formic acid (●); oxalic acid (△); (c) glyoxal (●); formaldehyde (□); acetaldehyde (△).

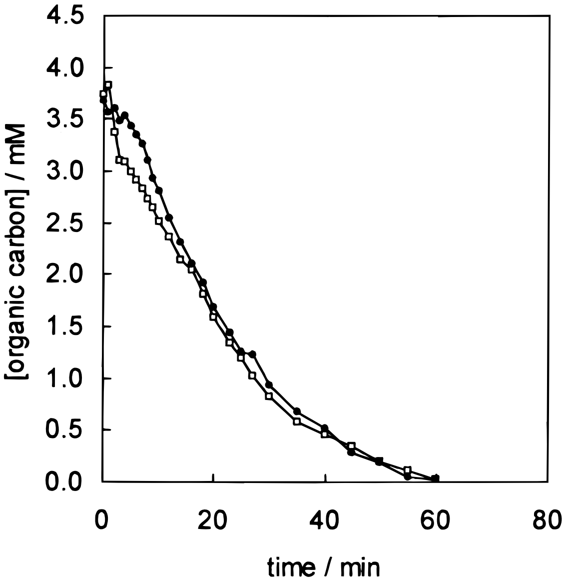

FIGURE 2. Total organic carbon (TOC) balance during the 1,4-dioxane treatment: TOC calculated from the experimental data on the 1,4-dioxane and its organic degradation products (□); TOC measured experimentally (●).

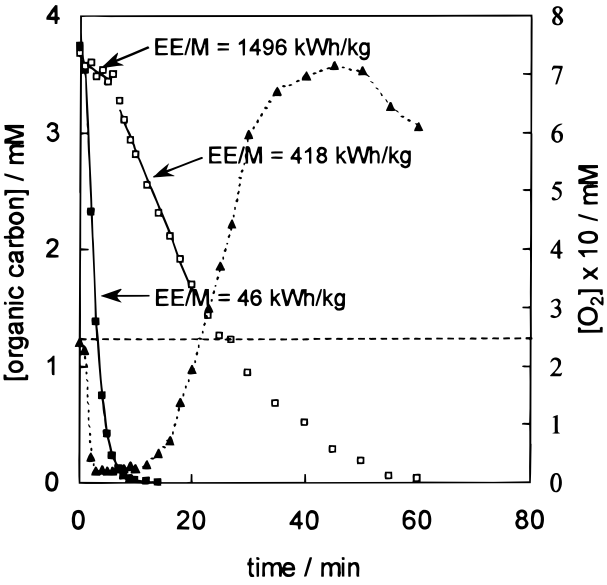

FIGURE 3. EE/M values as calculated during the TOC removal: TOC in 1,4-dioxane (■); TOC in the treated solution (□); oxygen concentration (▲); the oxygen level in air saturated conditions (- - -). The solid lines correspond to the linear regression for the zero order kinetics decay of TOC.

The dynamics of the system, consisting of the initial reagents (1,4-dioxane and H_2O_2) and the intermediates generated toward the complete destruction of each component, is governed not only by the O_2 and H_2O_2 concentrations in the solution, but also by the rate constants of various compounds with $^{\bullet}OH$ radicals. In the case of carboxylic acids, the pH plays an important role as well because, usually, their protonated forms react with $^{\bullet}OH$ radicals at different rate constants than the unprotonated ones.

1,4-Dioxane is removed rapidly from the system because of its high rate constant for reaction with $^{\bullet}OH$ radicals. The rate constants for the 1,2-ethanediol mono- and diformate esters are not known, but they are probably quite small, considering the slow decay observed for these esters in the solution (Figure 1a). Regarding formic acid, it reaches quite a high concentration in solution (Figure 1b), despite its high rate constant [3.2×10^9 M^{-1} s^{-1} (*42*)] with hydroxyl radicals, which indicates that it is continuously generated in the system within the first 20−25 min irradiation.

H_2O_2 (15 mM) was chosen as an initial concentration, because at that level, an optimum rate of 1,4-dioxane decay is obtained and a complete mineralization of any other organic intermediates generated in the studied system was achieved.

During the irradiation period, H_2O_2 follows zero-order kinetics (see Figure 1a) at a rate considerably lower [$(4.52 \pm 0.02) \times 10^{-6}$ M s^{-1}] than that for the photolysis of H_2O_2 alone [$(6.60 \pm 0.02) \times 10^{-6}$ M s^{-1}].

Total Organic Carbon (TOC) Time Profile during Irradiation. As shown in Figure 2, the total organic carbon concentration determined experimentally by TOC analysis is in good agreement, within experimental error, with that calculated from the sum of the carbon concentrations in the organic compounds identified and measured in the studied system during the irradiation period. This finding confirms that all major intermediates have been detected and quantified.

The TOC level by the end of the irradiation period confirms that the UV/H_2O_2 treatment of 1,4-dioxane solutions leads to the complete mineralization of any organic compounds present in the irradiated system, which is also consistent with the pH measured at the end of the experiment.

When studying the pollutant removal from contaminated water, it is important to consider both economic and environmental factors, the latter referring to the complete removal of TOC from the investigated system. Figure 3 gives a comparison between the electrical energy per mass (EE/M) values as calculated for organic carbon removal from 1,4-dioxane and the whole irradiated system, respectively. In this case, the EE/M is defined as the electrical energy in kilowatt hours required to bring about the degradation of 1 kg of contaminant carbon in the polluted water (*43*).

The removal of 1,4-dioxane requires only 46 kW h/kg of C due to its high reactivity toward $^{\bullet}OH$ radicals, while the removal of TOC follows zero-order kinetics in two stages, requiring much higher electrical energy input. During the first 5−7 min of irradiation, 1,4-dioxane is completely removed, but the TOC decreases only slightly, indicating that byproducts are formed and converted from one into the other with O_2 consumption. Accordingly, the EE/M has a high value. After the 1,4-dioxane removal, the intermediates compete efficiently with hydrogen peroxide for $^{\bullet}OH$ radicals, the oxygen level in the solution increases, and the TOC decreases more rapidly. Accordingly, the EE/M decreases.

Mechanism of 1,4-Dioxane Degradation Sensitized by the Photolysis of H_2O_2. We propose a mechanism (Schemes 1−8 and the discussion below) that aims to explain the experimental data discussed above and those obtained from the UV/H_2O_2 treatment of individual components (byproducts) identified in the studied system.

Initial Stages of the Degradation of 1,4-Dioxane. The initial degradation step, following the photochemical generation of reactive $^{\bullet}OH$ radicals (Scheme 1, reaction 1), is the attack on the 1,4-dioxane molecules (**1**) with H-abstraction leading to the 1,4-dioxanyl radical (**2**):

The 1,4-dioxanyl radicals (**2**) react with oxygen by a diffusion-controlled process forming peroxyl radicals (**3**). Fragmentation of **2** by β-cleavage (*44*) or by reaction with H_2O_2 at a rate constant of 3×10^4 M^{-1} s^{-1} (*45*) is very unlikely in the presence of oxygen. Generally, peroxyl radicals undergo head-to-head termination reactions with rate constants of ~10^9 M^{-1} s^{-1} in aqueous solutions (*46*), and the resulting tetroxide (**4**) decomposes to form molecular oxygen and α-oxyl radicals (**5**). Nese et al. (*47*) also claim that this reaction dominates over alternative reactions involving the formation of 1,4-dioxane-2-one or 2-hydroxy-1,4-dioxane. Furthermore, we have no experimental evidence for products such as these. On the other hand, an electrocyclic process leading to H_2O_2 and two carbonyl compounds (*48*) or disproportionation leading to oxygen, a 2-hydroxy alcohol and the corresponding carbonyl compound [Russell mechanism (*49*)], seems to be unlikely in the case of tetroxide derived from 1,4-dioxanyl peroxyl radicals considering the stereochemical hindrance.

The α-oxyl radical (**5**) derived from 1,4-dioxane appears to be the precursor of the primary major intermediates identified. This radical can undergo either an intramolecular reaction, in which the oxyl oxygen abstracts a hydrogen atom from the α′-C position followed by fragmentation (Scheme 2) or ΔC−C splitting at the α-C position (Scheme 3).

SCHEME 1. Initial Stages of the Degradation of 1,4-Dioxane

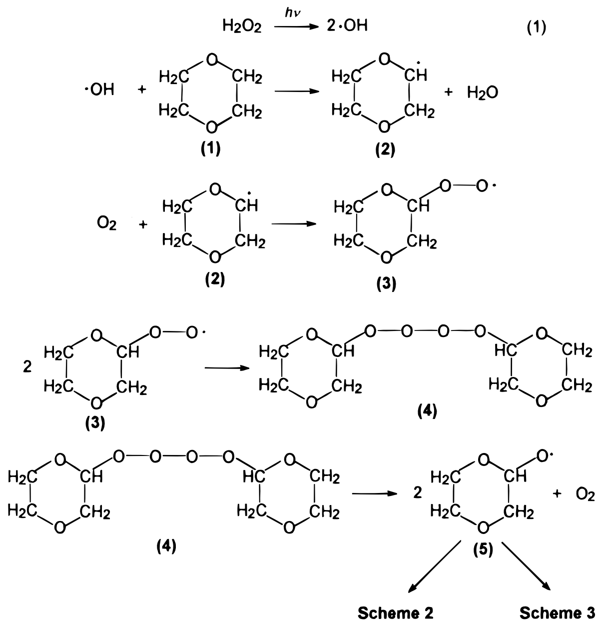

SCHEME 2. Reaction Pathways to and from Methoxyacetic Acid

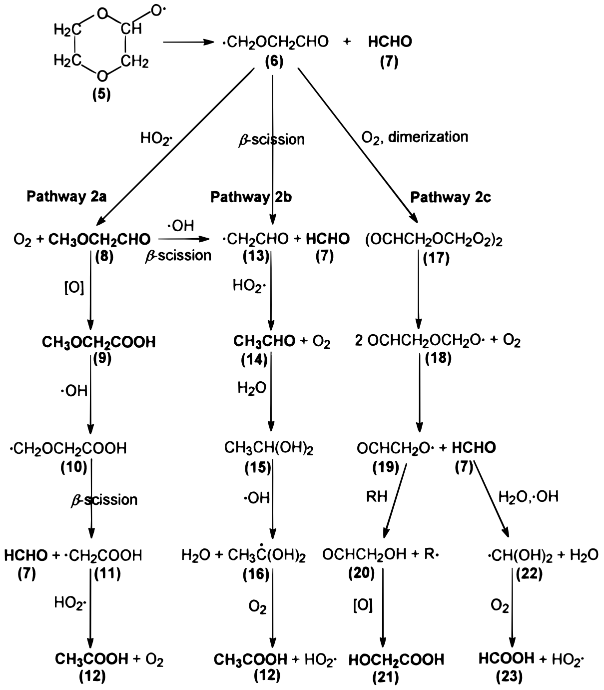

SCHEME 3. Reaction Pathways of the Generation of 1,2-Ethanediol Formate Esters

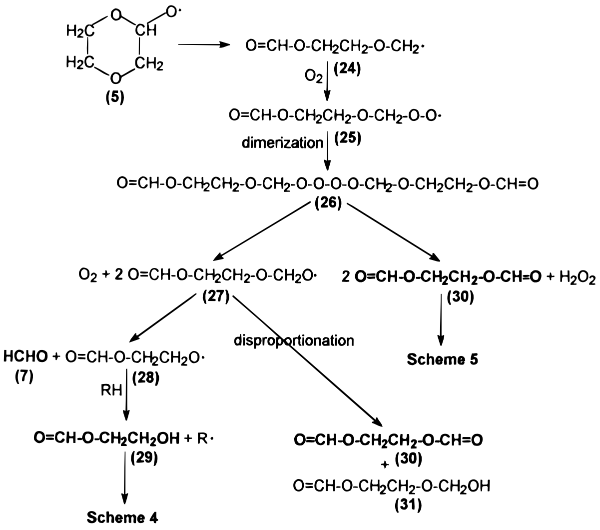

SCHEME 4. Reaction Pathways of the Degradation of 1,2-Ethanediol Monoformate

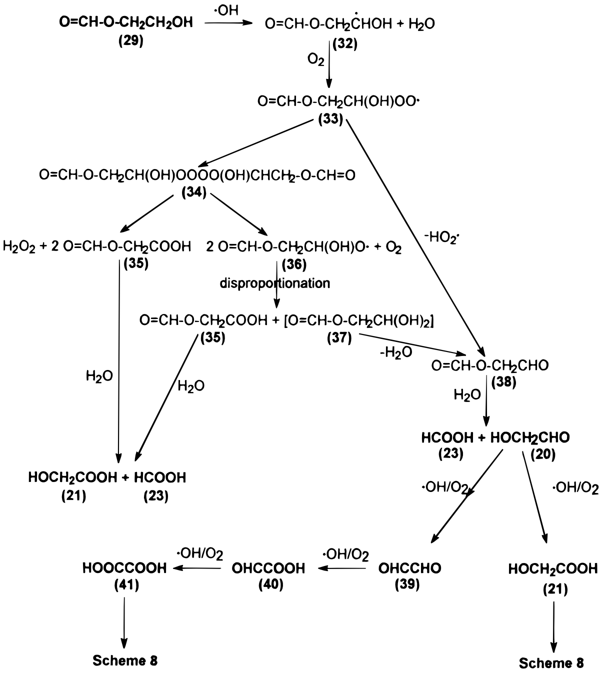

Depending on the route followed, either methoxyacetic acid (**9**) and fomaldehyde (**7**) or mono- and diformate esters of 1,2-ethanediol (**29** and **30**) and formaldehyde (**7**) are generated. According to the experimental concentrations determined for these organic compounds, the latter route seems to be favored.

Reaction Pathways to and from Methoxyacetic Acid. The generation of "methyl" groups in, for example, methoxyacetic acid or acetic acid requires, in our view, the "reduction" of an $RCH_2^{\bullet}$ type of radical. Although the concept is somewhat speculative, we consider that $HO_2^{\bullet}$ is the only effective reducing agent available. The reduction of **6** by $HO_2^{\bullet}$ radicals is expected because $HO_2^{\bullet}$ has both oxidizing and, particularly, reducing properties (*48*). The standard reduction potentials involving the $HO_2^{\bullet}/O_2^{\bullet -}$ species in water (vs NHE; O_2 at 1 atm) are $E°(O_2, H^+/HO_2^{\bullet}) = -0.05$ V (pH 0) and $E°(O_2/O_2^{\bullet -}) = -0.33$ V (pH 7) (*50*). The hydroperoxyl radical $HO_2^{\bullet}$ has a pK_a value of 4.8 (*51*), so that, considering the pH values reached in the treated system, it exists primarily in the protonated form. Moreover, due to the strong depletion of oxygen within the first few minutes of irradiation (reaching concentrations as low as ~0.02−0.01 mM), the $HO_2^{\bullet}$ radicals, which also may attain levels of ~0.01 mM, can compete with O_2 for $RCH_2^{\bullet}$ type carbon-centered radicals. The $HO_2^{\bullet}$ radicals are generated in the system not only by photolysis of H_2O_2, but also by $HO_2^{\bullet}$ elimination from peroxyl radicals and by the reaction of $CO_2^{\bullet -}$ with O_2 in acidic media (see Scheme 6). The pathways involving reduction by $HO_2^{\bullet}$ are further

SCHEME 5. Reaction Pathways of the Degradation of 1,2-Ethanediol Diformate

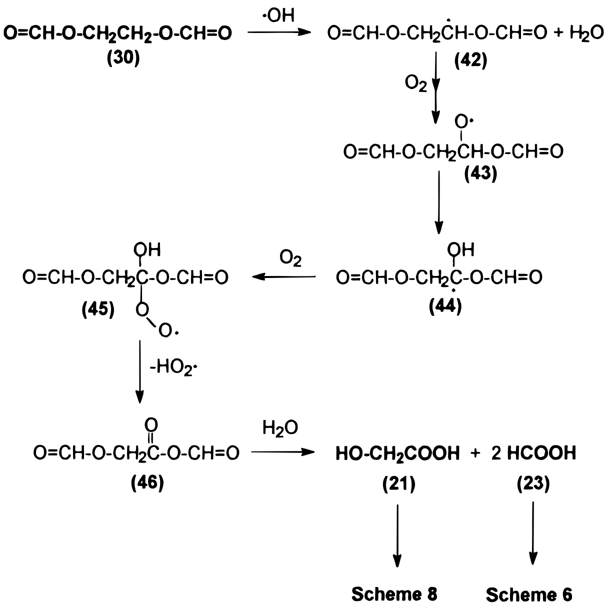

SCHEME 6. Degradation of Formic Acid

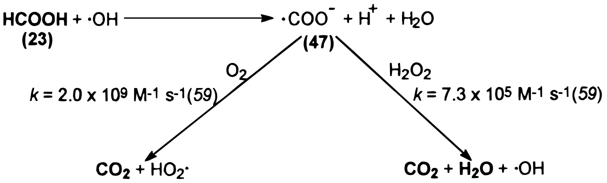

SCHEME 7. Reaction Pathways of the Degradation of Acetic Acid

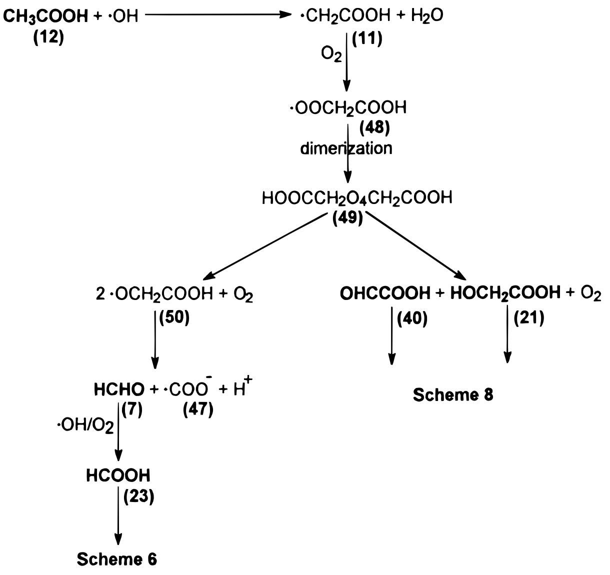

SCHEME 8. Reaction Pathways of the Degradation of Glycolic, Glyoxylic, and Oxalic Acids

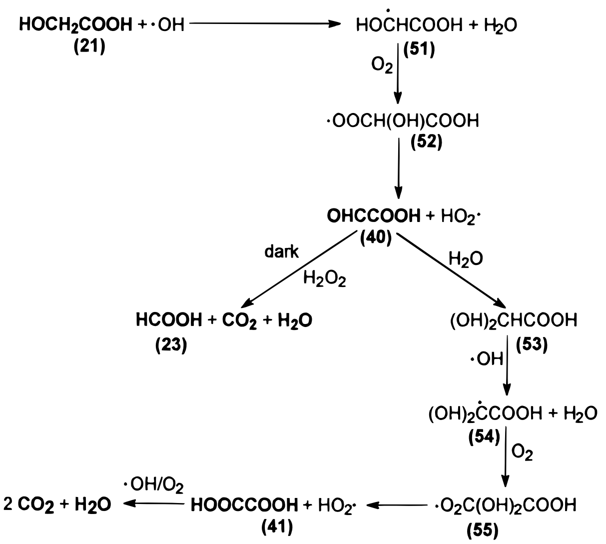

supported by the observation that methoxyacetic acid is not formed in the studied system in highly oxygenated solutions.

The carbon-centered radical (**6**) is hence either reduced by $HO_2^•$ radicals (pathway 2a) to methoxyacetaldehyde (**8**), which is further oxidized to methoxyacetic acid (**9**), or undergoes β-scission leading to acetaldehyde (**14**) as shown in pathway 2b.

Methoxyacetic acid (**9**) reacts rapidly with $^•OH$ radicals (pathway 2a, Scheme 2) by H-abstraction from the methyl carbon followed by fragmentation leading to formaldehyde (**7**) and formylmethyl radical (**11**). The latter goes to acetic acid (**12**) by a reduction reaction involving $HO_2^•$ radicals. We have discounted hydrogen atom abstraction from the β-carbon atom, since we assume that the adjacent oxygen to the methyl carbon atom makes that carbon atom electropositive and, hence, the favored site of attack.

Acetaldehyde hydrate (**15**) is further oxidized to acetic acid (see pathway 2b, Scheme 2). The reaction steps are initiated by $^•OH$ radical attack and involve peroxyl radical formation and spontaneous $HO_2^•$ elimination (*52*).

The carbon-centered radicals generated above probably also react with oxygen in parallel with the reduction reactions, but the occurrence of such oxidation reactions is less likely than reduction reactions when the concentration of oxygen is depressed. The subsequent oxidation reactions starting from the methoxyacetaldehyde radical would be expected to lead to glycolic acid, glyxoylic acid, and oxalic acid as major products, which have not been observed by a test irradiation experiment carried out on methoxyacetic acid in the presence of H_2O_2. The degradation of methoxyacetic acid using the UV/H_2O_2 system generated acetic and formic acids as the major byproducts and only a small amount of oxalic acid.

As mentioned above, to a small extent, the reaction steps of pathway 2c involving peroxyl radicals and tetroxide (**17**) formation might be considered as well. The oxyl radical (**18**) should undergo β-fragmentation releasing formaldehyde (**7**) and the oxyl radical of acetaldehyde (**19**), which is a strongly H-abstracting species from any RH type of molecule (e.g., 1,4-dioxane). The final products of this set of reactions are glycolic acid (**21**) and formaldehyde (**7**).

Formaldehyde is generated at very early times of irradiation and exists as a hydrate in aqueous solution, which is readily oxidized to formic acid (**23**).

Reactions Pathways to and from 1,2-Ethanediol Formate Esters. The generation of 1,2-ethanediol formate esters (Scheme 3) involves the most oxygen consuming processes. ΔC−C splitting of the 1,4-dioxan-α-oxyl radical (**5**) leads to radical (**24**). This radical primarily reacts with oxygen to form the corresponding peroxyl radical (**25**) and then dimerization to the tetroxide (**26**). According to the literature reports on the peroxyl radical chemistry (*48*, *53*, *54*), tetroxides generated from alkyl peroxyl radicals decompose either giving two oxyl radicals and molecular oxygen or through an electrocyclic process leading to H_2O_2 and two carbonyl compounds. Following these routes, the tetroxide (**26**) should lead either to the alkoxyl radical (**27**) or to 1,2-ethanediol diformate (**30**). The latter may also be formed as a result of disproportionation of the oxyl radicals (**27**) in the solvent cage. This type of reaction is well-known (*55*) and leads to the same products as the Russell mechanism (*49*), which represents another route of decomposition of tetroxides that does not involve free radicals as intermediates (*48*).

The oxyl radicals (**27**) can also undergo β-fragmentation. The alkoxyl radical (**28**) leads by H-abstraction from any RH type of compound (e.g., 1,4-dioxane) to 1,2-ethanediol monoformate (**29**).

Since we do not have any evidence for the presence of the alcoholic compound (**31**), but 1,2-ethanediol monoformate (**29**) has been detected, we consider that the disproportionation of (**27**) plays a very minor role in the reaction mechanism compared to the β-scission route. Moreover, if the branching ratio between the right branch (leading to **30**) and the left branch (leading to **27**) is approximately 3:1, as observed by von Sonntag and co-workers in the case of acetonylperoxyl radicals (*56*), a good agreement with the experimental concentration ratio of the two esters is obtained.

Radical **24** may also undergo β-scission leading to products such as ethyl formate and ethanol by a reduction pathway or to 1,2-ethanediol monoformate (**29**), formic acid and glycolaldehyde (**20**) by an oxidation pathway. We do not consider this route to be significant because we have not detected ethyl formate or ethanol, and there are other routes (see Scheme 3) to the other possible products.

1,2-Ethanediol monoformate (**29**) degrades slowly to glycolic (**21**) and formic (**23**) acids as major products. As the H-abstraction reaction takes place at the α-C, an oxidation mechanism can be assumed (Scheme 4).

The α-hydroxyalkylperoxyl radical (**33**) can both dimerize to tetroxide (**34**) or undergo a rapid $HO_2^•$ elimination reaction, which has been observed in the literature for peroxyl radicals derived from primary alcohols [$k \approx 10^7$ s^{-1}, (*54*)].

The acid ester **35** and the aldehyde ester **38** are unstable compounds, which undergo acid-catalyzed hydrolysis to glycolic (**21**) and formic (**23**) acids.

The aldehyde ester **38** can react with $^•OH$ radicals leading by subsequent reactions to glyoxal **39**, which has been identified as an intermediate in the investigated system and is a precursor of oxalic acid (**41**). The oxidation steps of glyoxal to oxalic acid are similar to those presented above for either formaldehyde or acetaldehyde, considering the hydrated molecules.

The $^•OH$ radical attack on the 1,2-ethanediol monoformate (**29**) may also take place at the β-C of the molecule leading to glycolic and formic acids as final products. Considering the high reactivity of primary alcohols toward $^•OH$ radicals, we propose that the $^•OH$ attack at the α-C is followed preponderantly.

The degradation of 1,2-ethanediol diformate (**30**) is also an oxygen-demanding process which is initiated by $^•OH$ radical attack. The degradation products are formic acid (**23**), glyoxal (**39**), and glycolic acid (**21**). Probably, the mechanism goes through an oxy radical (**43**) generated by H-abstraction followed by O_2 addition (Scheme 5).

It is important to mention that 1,2-ethanediol has not been detected as an intermediate, which suggests that the hydrolysis of its formate esters does not occur within the pH range generated under our experimental conditions.

Degradation Pathways for Formic, Acetic, Glycolic, and Oxalic Acids. Formic acid is a degradation product both of 1,4-dioxane and of some intermediates generated during the UV/H_2O_2 treatment of the investigated system. The rate constants of HCOOH/$HCOO^-$ for reaction with $^{\bullet}$OH radicals are as high as that for 1,4-dioxane. At very early irradiation times (1−3 min), the 1,4-dioxane concentration is still high enough to scavenge most of the $^{\bullet}$OH radicals generated by the direct photolysis of H_2O_2, but then, formic acid becomes an effective scavenger of $^{\bullet}$OH radicals. Literature reports (*21*, *57*, *58*) have emphasized the role of oxygen on the rate and the mechanism of the photooxidation of formic acid in aqueous solution in the presence of hydrogen peroxide. In our system, where the oxygen concentration is strongly depleted to $\sim 2.0 \times 10^{-5}$ M after the first few minutes of irradiation while the H_2O_2 concentration is still high (∼0.015−0.012 M), the formoyl radicals (**47**) generated in the H-abstraction reaction are undoubtedly involved in competitive reactions as shown in Scheme 6.

The generation of hydroxyl radicals in anaerobic systems through the reaction of $^{\bullet}$COOH radicals with hydrogen peroxide plays an important role in enhancing the rate of organic pollutant removal.

Experiments carried out on the degradation of acetic acid (**12**) by the UV/H_2O_2 process for similar concentration conditions as in the present study indicated only small amounts of glyoxylic and oxalic acids as intermediates. Therefore, we assume that the route involving the alkoxyl radical (**50**) is followed preponderantly (Scheme 7).

The same reaction products of acetic acid degradation either in pulse radiolysis studies (*59*) or by a UV/H_2O_2 treatment (*23*) have been reported in the literature.

Test experiments carried out on the oxidation of glycolic acid (**21**), initiated by $^{\bullet}$OH radical attack, indicated a very fast decay of glycolic acid with the generation of formic (**23**), glyoxylic (**40**) and oxalic (**41**) acids as byproducts toward a complete mineralization. The amount of oxalic acid generated was high, an observation which supports the above statements regarding the degradation pathways of acetic acid. The reaction steps approaching the degradation of these acids are given in Scheme 8.

Glyoxylic acid (**40**) undergoes both thermal and light-induced oxidation. The dark reaction leads to formic acid (**23**), whereas the light-driven one leads to oxalic acid (**41**). The high reactivity of glyoxylic acid in the presence of hydrogen peroxide explains the concentration of this compound at trace levels in the studied system.

Oxalic acid is the last detected intermediate and is generated both through the above reactions and by the oxidation of glyoxal (**39**). In the pH range measured during the exposure time, this acid exists mostly as hydrogen oxalate ion. Both glyoxal and hydrogen oxalate ion have low rate constants for reaction with $^{\bullet}$OH radicals, compared to the other intermediates detected in the system, which explains the time profile of oxalic acid. Its decomposition is mediated by reaction 2 with $^{\bullet}$OH radicals, when a direct mineralization takes place.

$$\mathrm{HOOCCOOH} + {}^{\bullet}\mathrm{OH} \longrightarrow \mathbf{CO_2} + \mathbf{H_2O} + {}^{\bullet}\mathrm{COOH} \qquad (2)$$

All the observed intermediates in the 1,4-dioxane treatment by the UV/H_2O_2 system in aqueous solution are weak absorbers of UV light. Considering the initial H_2O_2 concentration and its decay during the irradiation period, one can state that hydrogen peroxide is the strongest absorber of the UV light in the system, so that direct photolysis of the generated intermediates can be neglected. Thus, the oxidation and mineralization processes are strongly dependent on the $^{\bullet}$OH rate constants for the reaction of individual compounds, the relative concentrations of intermediates and the oxygen level in the solution.

Acknowledgments

This work was supported financially by a Collaborative Research and Development Grant jointly funded by the Natural Science and Engineering Research Council of Canada and Calgon Carbon Oxidation Technologies, Markham, Ontario, Canada. We are very grateful to Dr. Dave Budac for carrying out the mass spectroscopic measurements. We extend our thanks to Dr. Stephen Cater, Dr. Ali Safarzadeh-Amiri and Mr. Keith Bircher, P. Eng., of Calgon Carbon Oxidation Technologies for their helpful comments and support during the conduct of this research. The comments of the reviewers were highly appreciated.

Literature Cited

(1) Budavari, S.; O'Neil, M. J.; Smith, A.; Heckelman, P. E.; Kinneary, J. F. *The Merck Index,* 12th ed.; Merck & Co., Inc.: Whitehouse Station, NJ, 1996.
(2) U.S. Department of Health and Human Services, *Seventh Annual Report on Carcinogens*, 1994; PB95-109781, p 186.
(3) Heukelekian, H.; Rand, M. C. *Sewage Ind. Wastes* **1955**, *27*, 1040.
(4) Swope, H. G.; Kenna, M. *Sew. Ind. Waters Eng.* **1950**, *21*, 467.
(5) McGrane, W. In *Proceedings of the Sixth International Symposium on Chemical Oxidation Technology for the Nineties*; Vanderbilt University: Nashville, TN, 1996.
(6) Adams, C. D.; Scanlan, P. A.; Secrist, N. D. *Environ. Sci. Technol.* **1994**, *28*, 1812.
(7) Klecka, G. M.; Gonsoir, S. J. *J. Hazard. Mater.* **1986**, *13*, 161.
(8) Maurino, V.; Calza, P.; Minero, C.; Pelizzetti, E.; Vincenti, M. *Chemosphere* **1997**, *35*, 2675.
(9) Hill, R. R.; Jeffs, G. E.; Roberts, D. R. *J. Photochem. Photobiol. A: Chem.* **1997**, *108*, 55.
(10) Omura, K.; Matsuura, T. *Tetrahedron* **1968**, *24*, 3475.
(11) Koubek, E. *Ind. Eng. Chem., Process Des. Dev.* **1975**, *14*, 348.
(12) Mill, T.; Gould, C. W. *Environ. Sci. Technol.* **1979**, *13*, 205.
(13) Legrini, O.; Oliveros, E.; Braun, A. M. *Chem. Rev.* **1993**, *93*, 671.
(14) Sundstrom, D. W.; Weir, B. A.; Klei, H. G. *Environ. Prog.* **1989**, *8*, 6.
(15) Huang, C.-R.; Shu, H.-Y. *J. Hazard. Mater.* **1995**, *41*, 47.
(16) Shen, Y.-S.; Ku, Y.; Lee, K.-C. *Water Res.* **1995**, *29*, 907.
(17) Sheck, C. K.; Frimmel, F. H. *Water Res.* **1995**, *29*, 2346.
(18) Guittonneau, S.; De Laat, J.; Duguet, J. P.; Bonnel, C.; Dore, M. *Ozone Sci. Eng.* **1990**, *12*, 73.
(19) Benitez, F. J.; Beltran-Heredia, J.; Acero, J. L.; Gonzalez, T. *Water Res.* **1996**, *30*, 1597.
(20) Kawaguchi, H. *Chemosphere* **1993**, *27*, 577.
(21) Kawaguchi, H. *Chemosphere* **1993**, *26*, 1965.
(22) Karpel Vel Leitner, N.; Doré, M. *J. Chim. Phys.* **1994**, *91*, 503.
(23) Karpel Vel Leitner, N.; Dore, M. *Water Res.* **1997**, *31*, 1383.
(24) Stefan, M. I.; Hoy, A. R.; Bolton, J. R. *Environ. Sci. Technol.* **1996**, *30*, 2382.
(25) Sundstrom, D. W.; Klei, H. E.; Nalette, T. A.; Reidy, D. J.; Weir, B. A. *Hazard. Waste Hazard. Mater.* **1986**, *3*, 101.
(26) Wolfrum, E. J. In *Symposium on Environmental Applications of Advanced Oxidation Techniques*; EPRI & NSF: San Francisco, CA, 1993.
(27) Hirvonen, A.; Tuhkanen, T.; Kalliokoski, P. *Environ. Technol.* **1996**, *17*, 263.
(28) Hirvonen, A.; Tuhkanen, T.; Kalliokoski, P. *Water Sci. Technol.* **1996**, *33*, 67.
(29) Yue, P. L.; Legrini, O. *Water Poll. Res. J. Canada* **1992**, *27*, 123.
(30) Schuchmann, H.-P.; Bandmann, H.; von Sonntag, C. *Z. Naturforsch.* **1979**, *34*b, 327.
(31) Houser, J. J.; Sibbis, B. A. *J. Org. Chem.* **1977**, *42*, 2145.
(32) Kiwi, J. *J. Photochem.* **1977**, *7*, 237.
(33) Ausloos, P.; Lutz, C.; Schwarz, F.; Lias, S. G. *Radiat. Phys. Chem.* **1984**, *23*, 97.
(34) Mazzocchi, P. H.; Bowen, M. W. *J. Org. Chem.* **1975**, *40*, 2689.
(35) Schuchmann, H.-P.; von Sonntag, C. *J. Photochem. Photobiol. A: Chem.* **1990**, *52*, 97.
(36) Bilski, P.; Chignell, C. F.; Szychlinski, J.; Borkowski, A.; Oleksy, E.; Reszka, K. *J. Am. Chem. Soc.* **1992**, *114*, 549.

(37) Cater, S. R.; Brown, P. M.; Buckley, J. A.; Stevens, R. D. S. U.S. Patent No. 5,043,080, 1992.
(38) Murov, S. L.; Carmichael, I.; Hug, G. L. *Handbook of Photochemistry*, 2nd ed.; Marcel Dekker: New York, 1993; pp 299−305.
(39) Klassen, N. V.; Marchington, D.; McGowan, H. C. E. *Anal. Chem.* **1994**, *66*, 2921.
(40) Fung, K.; Grosjean, D. *Anal. Chem.* **1981**, *53*, 168.
(41) Nash, T. *Biochem. J.* **1953**, *55*, 416.
(42) Buxton, G. V.; Greenstock, C. L.; Helman, W. P.; Ross, A. P. *J. Phys. Chem. Ref. Data* **1988**, *17*, 513.
(43) Bolton, J. R.; Bircher, K.; Tumas, W.; Tolman, C. A. *J. Adv. Oxid. Technol.* **1996**, *1*, 13.
(44) Zimina, G. M.; Kosobutskii, V. S.; Petryaev, E. P.; Shadyro, O. I. *High Energy Chem.* **1986**, *20*, 171.
(45) Gilbert, B. C.; Norman, R. O. C.; Sealy, R. C. *J. Chem. Soc., Perkin Trans. 2* **1974**, 824.
(46) Schuchmann, M. N.; von Sonntag, C. *J. Phys. Chem.* **1982**, *86*, 1995.
(47) Nese, C.; Schuchmann, M. N.; Steenken, S.; von Sonntag, C. *J. Chem. Soc., Perkin Trans. 2* **1995**, 1037.
(48) von Sonntag, C.; Schuchmann, H.-P. *Angew. Chem., Int. Ed. Engl.* **1991**, *30*, 1229.
(49) Russell, G. A. *J. Am. Chem. Soc.* **1957**, *79*, 3871.
(50) Huie, R. E. In *Progress and Problems in Atmospheric Chemistry*; Barker, J. R., Ed.; World Scientific: Singapore, 1995; pp 374−419.
(51) Bielski, B. H. J.; Cabelli, D. E.; Arudi, R. L.; Ross, A. B. *J. Phys. Chem. Ref. Data* **1985**, *14*, 1041.
(52) Schuchmann, M. N.; von Sonntag, C. *J. Am. Chem. Soc.* **1988**, *110*, 5698.
(53) Ingold, K. U. *Acc. Chem. Res.* **1969**, *2*, 1.
(54) Bothe, E.; Schulte-Frohlinde, D. *Z. Naturforsch.* **1978**, *33*b, 786.
(55) Mendenhall, G. D.; Quinga, E. M. Y. *Int. J. Chem. Kinet.* **1985**, *17*, 1187.
(56) Zegota, H.; Schuchmann, M. N.; Schulz, D.; von Sonntag, C. *Z. Naturforsch.* **1986**, *41*b, 1015.
(57) Karpel Vel Leitner, N.; Dore, M. *J. Photochem. Photobiol. A: Chem.* **1996**, *99*, 137.
(58) Ogata, Y.; Tomizawa, K.; Takagi, K. *Can. J. Chem.* **1981**, *59*, 14.
(59) Schuchmann, M. N.; Zegota, H.; von Sonntag, C. *Z. Naturforsch.* **1985**, *40*b, 215.

Received for review July 18, 1997. Revised manuscript received February 6, 1998. Accepted February 17, 1998.

ES970633M